



Correlation of Alfvén Mach number with field aligned current, polar cap potential and dawn dusk electric field during Quiet and extreme solar wind conditions

Binod Adhikari^{a,c*}, Drabindra Pandit^{a,c}, Prashrit Baruwal^c, Opendra Thapa^a, Niraj Adhikari^a, Bidur Kaphle^a, Pratik Bhattarai^a, Narayan P. Chapagain^d & Sarala Adhikari^c

^aDepartment of Physics, St. Xavier's College, Tribhuvan University, Kathmandu 44600, Nepal

^bDepartment of Physics, Patan Multiple College, Tribhuvan University, Lalitpur 44700, Nepal

^cCentral Department of Physics, Tribhuvan University, Kathmandu 44600, Nepal

^dDepartment of Physics, Amrit Campus, Tribhuvan University, Kathmandu 44600, Nepal

^eDepartment of Environmental Science, Tri-Chandra College, Tribhuvan University, Kathmandu 44600, Nepal

Received: 12 December 2019; accepted: 2 September 2020

This paper has been performed to study the Alfvénic Mach number (M_A) in relation to Field Aligned Currents (FACs), Polar Cap Potential (PCV), Dawn Dusk Electric Field (E_y) during different geomagnetic conditions. The relations of M_A with FACs, PCV and interplanetary electric field (IEF)- E_y not solely dependent on any solar wind parameter but also associate with prior, main, and post conditions of geomagnetic storms. This study has shown that Prior to the arrival of interplanetary shock (IS), M_{MS} and M_A show good relationship with FAC, PCV, E_y , and solar wind parameters, as the space weather seems unperturbed. The positive correlations among the various parameters have obtained due to the merging of two different interplanetary coronal mass ejections (ICMEs) driven solar storms and consequential intense southward interplanetary magnetic field. The negative relationships among the selected parameters may have been due to the slow recovery of the IMF-Bz component. This study indicate that the preceding solar winds could be associated on the variance of M_A of a geomagnetic event, in turn might have its effects on FACs, PCV, E_y and in other solar wind parameters.

Keywords: Geomagnetic conditions, Field aligned currents, Polar cap potential, Dawn dusk electric field, Alfvén Mach number

1 Introduction

The solar wind is a magnetized plasma of charged particles, viz alpha particles, protons, electrons, etc. that flows outward from the Sun¹. When the solar wind magnetic field interacts with Earth's magnetic field, the excitation of the movement of electric current increases on increasing energies, in the magnetospheric-ionospheric (MI) system, result in geomagnetic storms, sub-storms, and aurora²⁻³. One aspect of the interaction of the solar wind and embedded interplanetary magnetic field (IMF) with the terrestrial magnetosphere is the generation of currents, geomagnetically-aligned electric currents, at high latitudes in the ionosphere and magnetosphere called Field Aligned Currents (FACs)⁴.

High altitude region (R1) and low altitude (R2) of FACs electronically couple the magnetospheric and ionospheric plasma and release the stress applied on the outer magnetospheric plasma to the

ionosphere and upper atmosphere⁵⁻⁷. During the dayside magnetopause reconnection, R1 and R2 become more significant and this mechanism is the major driven internal process related to magnetic storm/sub-storm. Large FACs are associated with polar regions that spans variation in polar cap potential due to reconnection process, when magnetic field lines intervene with IMF, on the dayside magnetosphere and in the magnetotail. For PCV in detail, references are herein⁸⁻¹³. PCV is crucial for delineation of the coupled magnetosphere-ionosphere system^{12,14}.

The E_y component of interplanetary electric field (IEF), $E_y = (V_{sw})_x \times IMF(Bz)$ maps down to the ionosphere as a convection E_y field. Under southward IMF Bz conditions, when the geomagnetic field merges with the IMF, a dawn-to-dusk convection E_y field is formed due to the R1-FACs closing in the high-altitude ionospheric dynamo region that can modify the orbits of charged particles by shifting them towards the dawn sector¹⁵⁻¹⁶.

*Corresponding author (E-mail: binod.adhi@gmail.com)

Alfven Mach number (M_A) characterizes the strength of the magnetic field. It is given as $\frac{V_{sw}}{V_A}$; where V_{sw} is solar wind velocity and V_A is Alfven speed, the speed with which hydrodynamic waves can propagate¹⁷. Sub-Alfvenic M_A (<1), the magnetic field lines shape the plasma whereas super-Alfvenic (>1) conditions, it is the opposite. Sub-Alfvenic M_A corresponds to a strong magnetic field while a super-Alfvenic M_A corresponds to a weak magnetic field¹⁸. Furthermore, when the solar wind M_A is high then thermal plasma forces dominate but when it is low, magnetic forces dominate. The coupling efficiency, ratio of output to input into M-I system, increases as a function of M_A ¹⁹. Iijima and Potemra²⁰ and Kasranetal²¹ have deduced a linear relation between large-scale FACs and V_{sw} . Similarly, PCV has also been found to be related to V_{sw} . Furthermore, Wilder *et al*²² found an anti-correlation of the dawn FAC strength with both the M_A and the SYM-H index. Adhikari *et al*²³ estimated the FAC and PCV values, their observed relationship, good positive correlation, validates the occurring of physical mechanism as FAC leads PCV. However, there has been less or no effort to find the relation of M_A to FAC, PCV, and Ey.

The drastic variation in an interaction of solar wind, due to low or high Mach number, with magnetosphere rendered a behavior of CME; however, geo-effective CMEs tend to have low (in average) Mach number. With the fall in Alfven M_A , the magnetic force as a flow rises; shows anti-correlation²⁴⁻²⁵. Furthermore, Borosky and Denton²⁶ found similar result for magnetic cloud associated with CMEs. The magnetosonic and Alfven Mach numbers relation is: $M_{MS} = V_{sw}/(V_s^2 + V_A^2)^{1/2}$ and $MA = V_{sw}/V_A$ respectively (where V_s, V_A , and V_{sw} are sonic, Alfven speeds, and Solar wind speed). During magnetic clouds, M_A and M_{MS} are even closer to each other (usually in the low Mach number regimes); these are characterized by unusually low temperatures²⁷. Lower bound of ($M_{MS} \geq 6.9$) for solar cycle (SC) 24 is larger in comparison with SC 22 and SC 23.

Fairfield *et al*²⁸ observed distant bow shock locations unraveling a much thicker magnetosheath during low Mach number regime. Upstream M_A shows Good agreement with bow shock²⁹. Wang, J. *et al*³⁰ found sunward movement of subsolar bow shock with increase in IMF Bz field strength and decrease in M_{MS} solar wind. Magnetic clouds are featured with

low M_A . Also, the higher the M_A value, slower is the sunward flow; no sunward flow is expected for $M_A > 3.26$. Furthermore, decrease in M_A value (low Mach number) hint of an expansion of bow shock surface; however, high $Ma > 25$ shocks are very rare in near earth environment. Some of such unusual cases were observed in this paper.

As we know, M_A is calculated from Band V_{sw} . Despite this, we have carried out our analysis to examine the variation of patterns during the quiet and extreme solar wind conditions. Since these parameters determine the change in the value of FAC, PCV, and IEF-Ey, there must be a direct relation between the M_A and the parameters of FAC, PCV, and IEF-Ey. In this study, our aim is to investigate the relation of M_A with FACs, PCV, and IEF-Ey under different solar wind conditions. Furthermore, our study includes the effect of preceding solar wind on the M_A of the geomagnetic condition, which if studied further would help to explain the unusual behavior observed in various parameters during the geomagnetic storms.

2 Dataset and Methodology

Our database consists of 1-minute resolution IMF-B and its southward component (B_z) (nT) and the various solar wind parameters such as V_{sw} (km/s), proton density (N_{sw} ; i^+/cm^3), temperature (T_{sw} ; K), and flow pressure (P_{sw} , nPa) and Alfven Mach Number (M_A) provided by the Omni Data Explorer. Three different types of events: a quiet, ICME driven, and a co-rotating interaction region (CIR) driven events fall under this database for years from 2001-2005. We adopted Iijima and Potemra²⁰ and Moon³¹ method to estimate the values of FAC, PCV, and dawn-dusk IEF-Ey respectively as:

$$FAC = 0.328 \sqrt{\sqrt{n_p} V_{sw} B_T \sin \frac{\theta}{2}} + 1.4 \quad \dots (1)$$

and

$$PCV = V_{sw} B_T \sin^2 \left(\frac{\theta}{2} \right) \times 7R_e \quad \dots (2)$$

In these equations, n_p is the solar wind density (n/cc), V_{sw} is the solar wind speed (km/s), B_T is transverse IMF (nT); $B_T = \sqrt{B_y^2 + B_z^2}$ and θ represents the angle between the Earth's magnetic field and the total IMF vector $\theta = \cos^{-1} \left(\frac{B_z}{B} \right)$.

In Eq (2) l_o is the effective length of the X line in a schematic which is empirically determined as $l_o=7R_E$, where R_E is the radius of Earth (6.48×10^6 m).

In addition, we studied the cross correlation between the Alfvénic M_A and different solar wind parameters like IMF-B, IEF-Ey and Vsw, and other parameters such as FACs, PCV, and SYMH during the events. This methodology offered a clear insight into the relation between these parameters during the periods investigated.

3 Results and Discussion

In this section, we discuss the Alfvénic Mach number in relation to field aligned currents, polar cap potential, dawn dusk electric field during the quieted day and geomagnetic storms.

Event-1: 23 December 2005 (The quietest day)

Quiet days (Q days) are the geomagnetically least disturbed days with Kp (not included in plots) values less than 3 and insignificant fluctuation in geomagnetic indices like AE and SYM-H). Figure 1 depicts the unperturbed state of the MI system; no prior, main, and post event are separately observed for 23rd December 2005. Fifth panel from top, shows the minimum value of 25 (10^4 K) for temperature while SYM-H index and IMF Bz varied within ± 5 nT. The solar wind parameter values, from panel 3-6, show gradually decreasing trend towards night side. The overall variation in data sets show the geomagnetically quiet event.

In Fig. 2, the variation in AE index value reached the maximum of ~ 75 nT, while negligible variation was observed on Alfvénic M_A , FACs, PCV, and dawn-to-dusk IEF Ey. The value of M_A reached the maximum of ~ 28 (>25) at ~ 3 UT and remained consistent for 6 UT- 18 UT³²; however, the average magnetic field (B) in Fig. 1 dropped down to minimum value of 2 nT and SYM-H value to 1 nT. The value of FAC also ranged from 1.5 to 3 amp. The values of PCV and IEF Ey ranged between 1 to ~ 3 kV and between ~ 1.5 to ~ 1 mV/m respectively. The fluctuation in M_A , FAC, PCV values on dayside was slightly higher than that with night side due to the consequences of solar wind parameters. The low value of FAC was due to the less interaction of IMF with the geomagnetic field that resulted in a decrease in plasma movement through the magnetosphere and a decrease in the electric currents³³⁻³⁴.

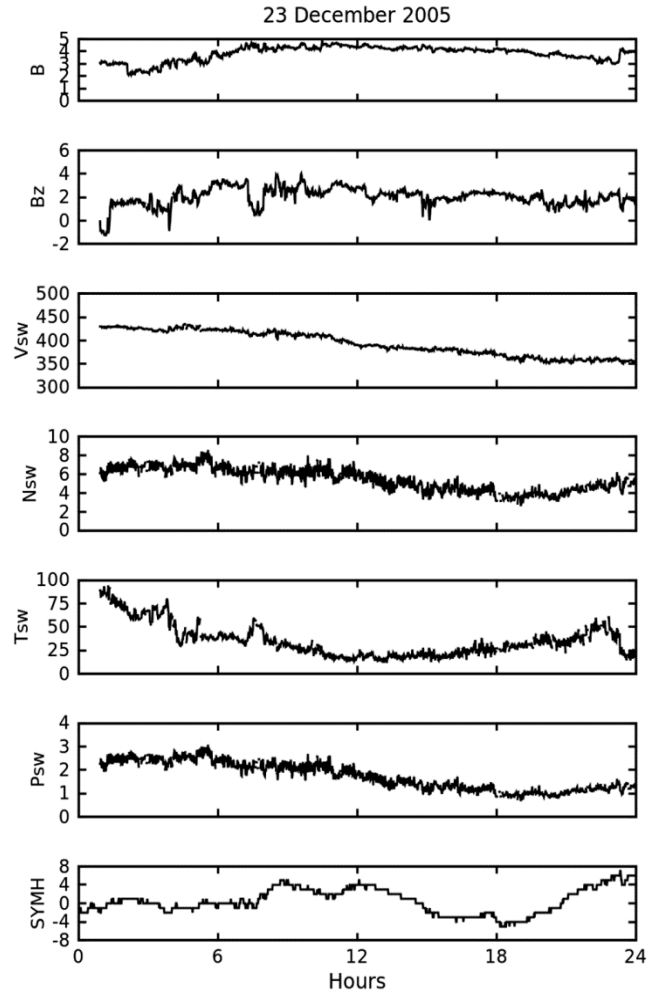


Fig. 1 — Represents the variation in IMF components and solar wind parameters observed on 23 December 2005. From top to bottom: (a) IMF magnitude (B; nT), (b) southward component of IMF (Bz; nT), (c) velocity of solar wind (Vsw; km/s), (d) density of solar wind (Nsw; i^+/cm^3), (e) temperature of solar wind ($10^4 T_{sw}$; K), (f) flow pressure of solar wind (Psw; nPa), and (g) SYMH index (nT).

Event-2: 31 March 2001 (ICME driven)

Figure 3 depicts the fluctuation in the IMF components and solar wind parameters during the ICME driven storm that occurred on 31 March 2001. The impingement of solar wind with bow shock of Earth can be identified with the sudden increase in negative SYM-H value. Sudden abrupt increase in solar wind parameters shows the flow and deflection of charge particles with the compression magnetosphere. The prior storm phase started at ~ 0100 UT and lasted till 0300 UT, followed by the abnormal short lived four swings showing negative IMF Bz excursion can be responsible for intense superstorms. During main storm phase, Vsw and IMF

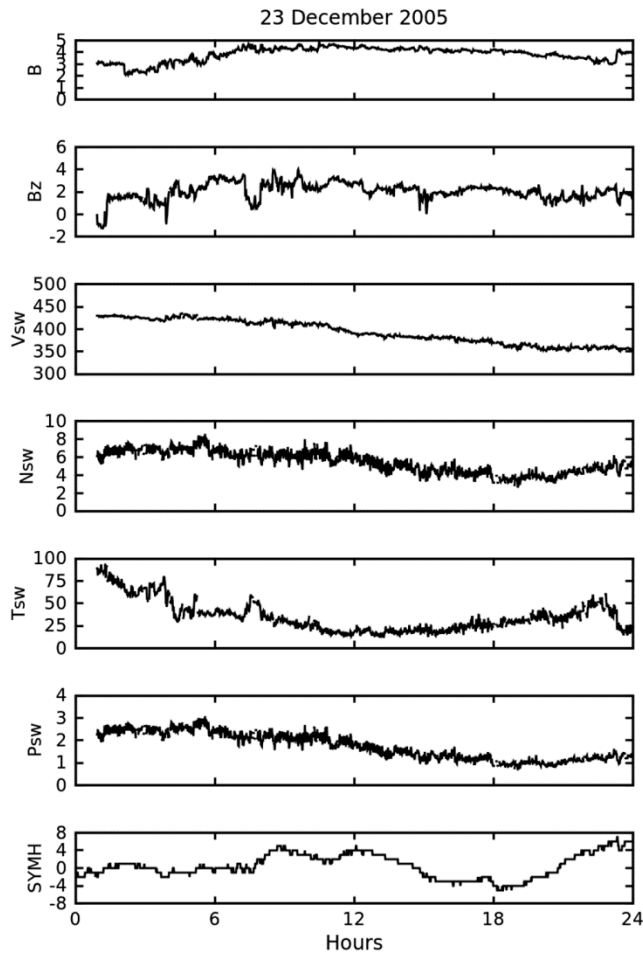


Fig. 2 — The different parameters are shown for 23 December 2005. From top to bottom: (a) Alfvén Mach number (M_A), (b) magnetosonic Mach number (M_{ms}), (c) field aligned current (FAC; amp), (d) polar cap potential (PCV; kV), (e) dawn dusk electric field (EFY; mV/m), (f) AE index (nT), and (g) SYMH index (nT).

B follow a similar pattern. The negative maximum IMF B_z value (~ -40 nT) slowed down the recovery phase; however, the SYM-H index attains its maximum value of -440 nT at ~ 0800 UT. The gradual recovery phase occurs during the post storm event.

Figure 4 shows the variation in estimated parameters, AE, and SYMH index (identical to Fig. 3 in the bottom panel). The second row from the bottom shows the AE index, which ranges from 100 nT to 2400 nT. The fluctuation of AE is irregular with a maximum value at about ~ 1700 UT indicates the precipitation of charged particles glowing the ionosphere. The third, fourth, and fifth panels from top show the line plots of FACs, PCV and dawn-to-dusk IEF E_y . These show a similar pattern of

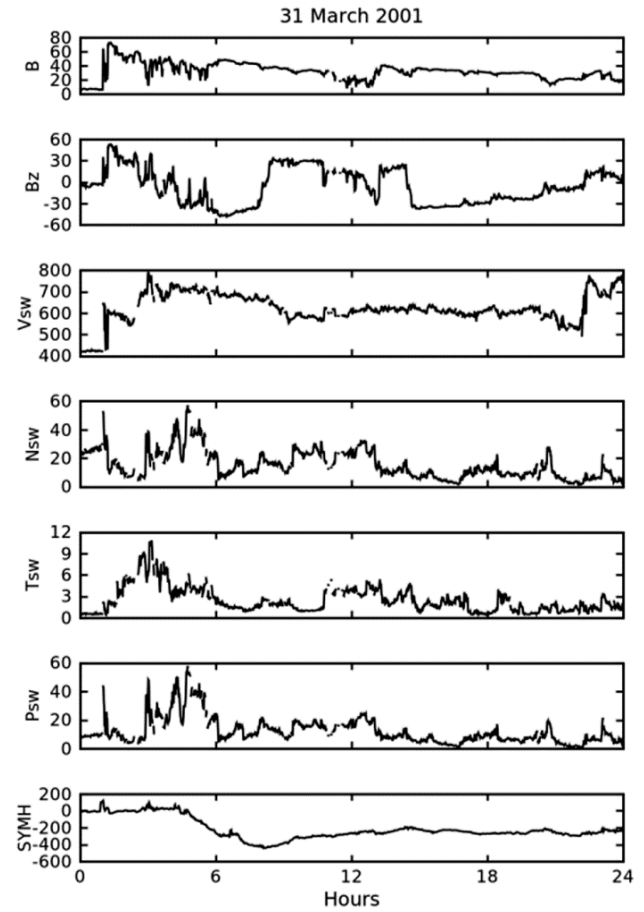


Fig. 3 — Represents the variation in IMF components and solar wind parameters observed on 31 March 2001. From top to bottom: (a) IMF magnitude (B; nT), (b) southward component of IMF (B_z ; nT), (c) velocity of solar wind (V_{sw} ; km/s), (d) density of solar wind (N_{sw} ; i^+/cm^3), (e) temperature of solar wind ($10e5$, T_{sw} ; K), (f) flow pressure of solar wind (P_{sw} ; nPa), and (g) SYMH index (nT). At M_A maximum, the solar wind velocity, temperature, density

variations because they hinge on the strength of solar wind-magnetosphere interactions³³. This shows that the FACs, PCV and IEF E_y are linearly correlated to each other. For intense superstorms, the average value of IEF E_y is ~ 23.5 mV/m³⁵. The value of M_A ranges from 1 to 20 show satisfactory data whereas the value of M_{ms} ranges from 1 to 8 such that M_A and M_{ms} have shown direct relation to each other.

The fluctuations in FAC and PCV are associated with the swift of southward IMF B_z component responsible for a change in the electric field of cross-magnetosphere³⁶. Positive in SYMH value depicts the compression phase of geomagnetic storm with the flow of eastward magnetopause current³⁷.

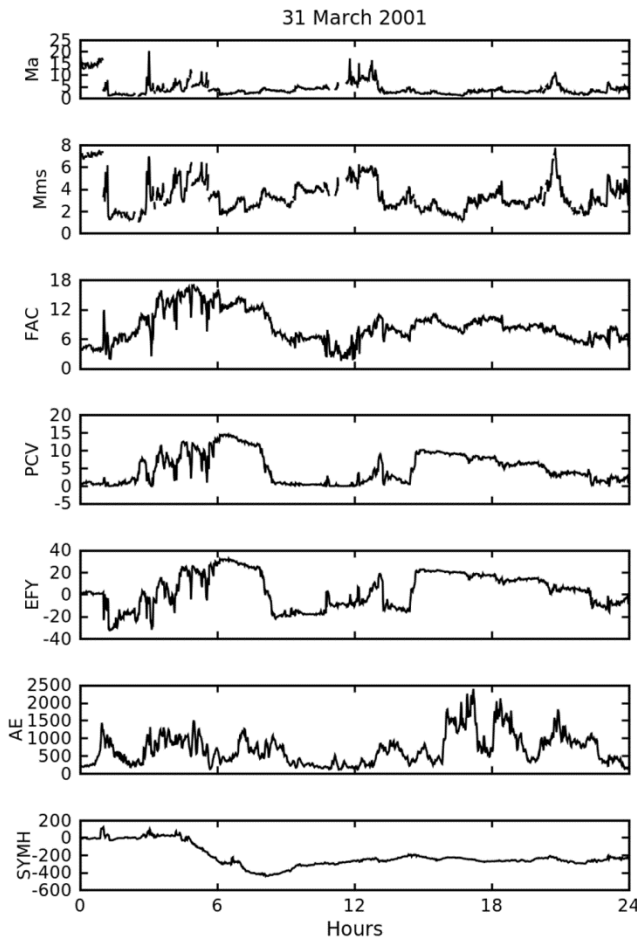


Fig. 4 — The different parameters are shown for 31 March 2001. From top to bottom: (a) Alfvén Mach number (M_A), (b) magnetosonic Mach number (M_{ms}), (c) field aligned current (FAC; amp), (d) polar cap potential (PCV; kV), (e) dawn dusk electric field (EFY; mV/m), (f) AE index (nT), and (g) SYMH index (nT).

Event-3: 20 November 2003 (ICME event)

In Figs 5 and 6, we can observe the variation in the various parameters associated with the ICME event occurred at 20 November 2003. The rises and falls in the various parameters help us deduce the underlying condition of M_A , FAC, PCV, and dawn-to-dusk IEF E_y derived from the Interplanetary and solar wind parameters. At around 09:00 UT, sudden increase in solar wind parameters in Fig. 5 marked the commencement of the storm. Rapid fluctuations of parameters in both the Figs 5 and 6, during 09:15 UT till 11:15 UT, for 2 hours of interval between first northward IMF- B_z excursion and the slight recovery phase before the second negative IMF B_z excursion was observed; however, the average magnetic field B shows gradual increasing trend reaching the maximum value of ~ 60 nT at 15:30 UT with the

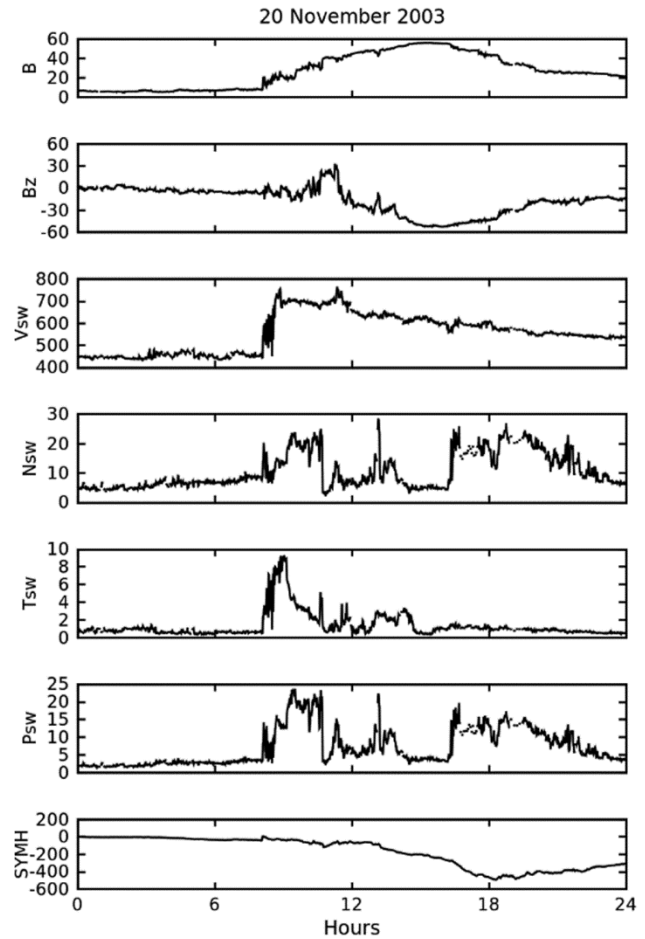


Fig. 5 — Represents the variation in IMF components and solar wind parameters observed on 20 November 2003. From top to bottom: (a) IMF magnitude (B ; nT), (b) southward component of IMF (B_z ; nT), (c) velocity of solar wind (V_{sw} ; km/s), (d) density of solar wind (N_{sw} ; $i+/cm^3$), (e) temperature of solar wind ($10e5$ Tsw; K), (f) flow pressure of solar wind (P_{sw} ; nPa), and (g) SYMH index (nT).

decreasing SYM-H (symmetric-H) value till 18:00 UT. The multiple peak values of AE during the storm, indicates the ongoing auroras. During the storm, FAC ranged from 3 to 15 amp while V_{sw} ranged from 400 km/s to 750 km/s. The variation pattern of FAC is similar to that of V_{sw} . The findings of Iijima and Potemra²⁰ and, regarding the existence of a linear relation between FAC and V_{sw} , support our finding. In addition, anti-relationship between IMF B_z and IEF E_y was observed: negative IMF B_z excursion (max. ~ 50 nT) deflects towards southward, meanwhile, an IEF E_y (max. ~ 35 mV/m) increases eastward. This leads to an increase in magnitude of ionospheric Cross PCV which establishes a linear correlation between PCV and V_{sw} ³⁸⁻⁴⁰. During this event, the value of PCV varied between 0 and 15 kV.

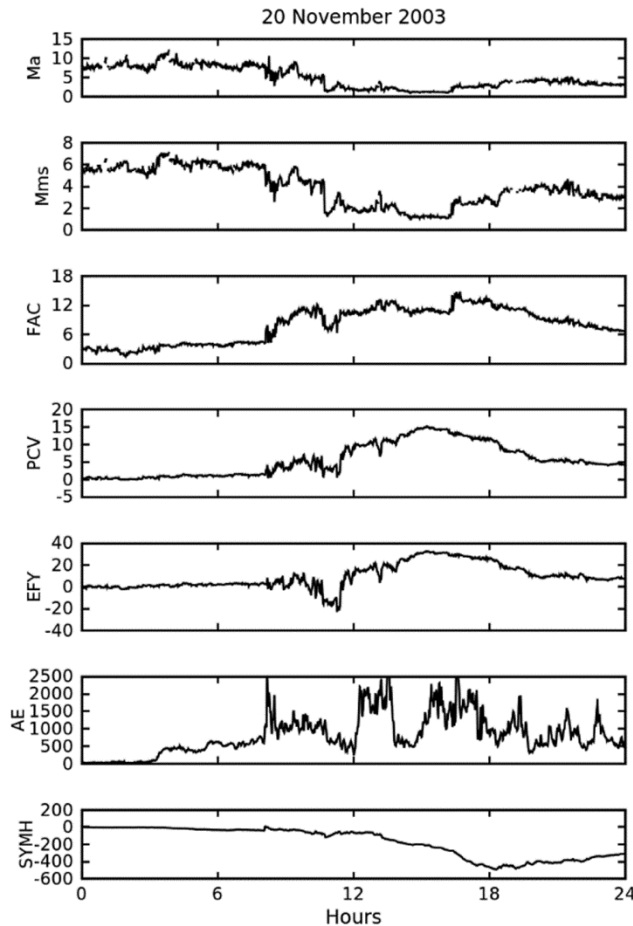


Fig. 6 — The different parameters are shown for 20 November 2003. From top to bottom: (a) Alfvén Mach Number (M_A), (b) magnetosonic Mach number (M_{ms}), (c) field aligned current (FAC; amp), (d) polar cap potential (PCV; kV), (e) dawn dusk electric field (EFY; mV/m), (f) AE index (nT), and (g) SYMH index (nT).

According to Chapman and Cairns¹⁷, when the value of solar wind velocity increases during the beginning of storm, the M_A also increases and shows the same fluctuation as V_{sw} throughout the disturbance period. Regarding this storm, as the solar wind increased, the value of M_A decreased that is completely the opposite of the observation of Chapman and Cairns¹⁷. This observed variability helps us conclude that an inverse relationship can also exist between V_{sw} and M_A during a strong super solar storm. Furthermore, as there is only a gradual or incomplete recovery noticed in the IMF-Bz after the storm, we believe this delay in the recovery may be the reason for the establishment of a negative relation between V_{sw} and M_A . In this storm and during its the main phase, there was a rapid and remarkable decrease in the IMF Bz component while it tried to

recover slowly after the storm main phase but did not recover completely by the end of this event. As the Alfvén M_A denotes the magnetic field strength, we conclude that this slow recovery of IMF-Bz was a responsible factor for the inverse relation of V_{sw} and Alfvén M_A observed.

As PCV, FAC, and IEF E_y are all directly proportional to V_{sw} , and IEF- E_y is inversely proportional to V_{sw} , we can conclude the existence of an inverse relation among PCV, FAC, and IEF E_y with M_A during this ICME driven solar superstorm.

Event-4: 15 May 2005 (CIR event)

Figures 7 and 8 depict the variation in interplanetary and solar wind parameters due to the CIR storm structure occurred at 15 May 2005. The storm commenced with the positive increment of SYM-H value, indicating the flow of current along the magnetopause due the rapid compression of bow shock. During the prior phase of ICME events (Figs. 3-6), there was an abrupt increment in solar wind parameters. However, in the case of CIR event in prior phase, there existed a gradual increment in solar wind parameters with the commencement of storm. In prior phase, the data show missing values but the SYM-H attends ~ 3 hours (03:00 UT to 06:00 UT) of positive increment value before the main phase of CIR event. This indicates that the large amount of energy was ejected in the magnetopause unlike during the ICME event. In addition, strong auroral effect with the AE minimum value of ~ 500 nT was observed. An abrupt increase in M_A value with minimum of 10 and maximum value of ~ 48 was observed, which is very rare in our solar space environment. The M_A values are vital for the characterization of collision less shocks. During the main phase of storm, the lowest value of SYM-H approximately -305 nT at $\sim 08:20$ UT was observed and thus classified as a major geomagnetic storm based on criteria suggested by Gonzalez *et al.*³. V_{sw} maintained the mean value of ~ 800 km/s throughout event. Meanwhile, P_{sw} fluctuated between ~ 2 nPa and ~ 58 nPa from 03:00 UT to 09:00 UT. The variation of FAC and PCV in CIR event is like earlier ICME events; however, during the post event, i.e., recovery phase the fluctuation in parameters showed negligible response. As such, we have a positive relation between V_{sw} and the variables of FACs, PCV and IEF E_y but these variables have a negative relation with M_A . Thus, we conclude the existence of

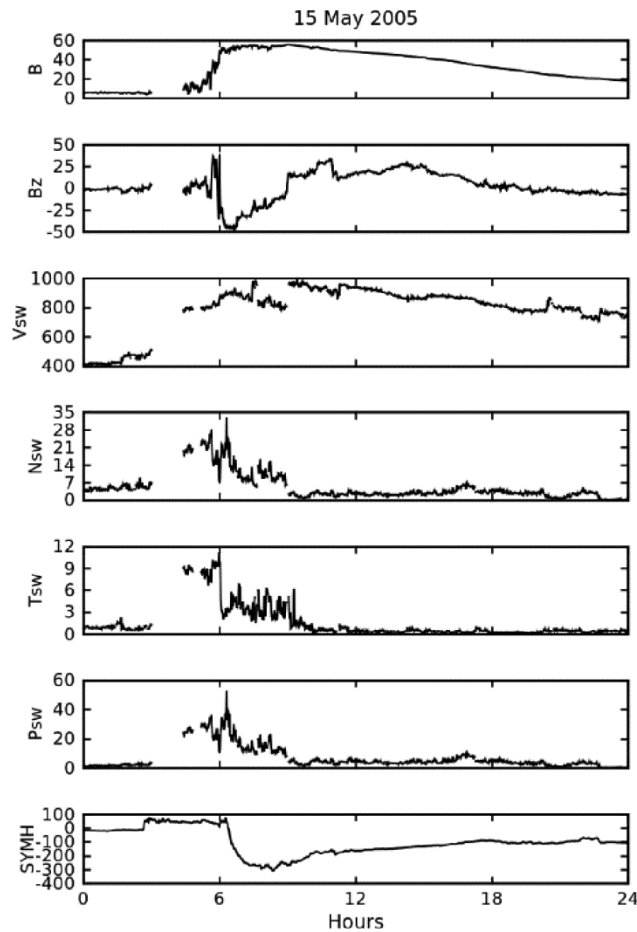


Fig. 7 — Represents the variation in IMF components and solar wind parameters observed on 15 May 2005. From top to bottom: (a) IMF magnitude (B ; nT), (b) southward component of IMF (B_z ; nT), (c) velocity of solar wind (V_{sw} ; km/s), (d) density of solar wind (N_{sw} ; $i+/cm^3$), (e) temperature of solar wind ($10e5$, Tsw; K), (f) flow pressure of solar wind (P_{sw} ; nPa), and (g) SYMH index (nT).

a negative relation between M_A and these variables (i.e., FACs, PCV and IEF E_y) during this storm.

Cross correlations

In Figs 9-12, the graphs of cross-correlation coefficient versus time in minutes are plotted. Cross correlation is the standard, multi-time scale, statistical tool that estimate time delay between two different time scale parameters as a function of time lag to draw new information⁴¹⁻⁴³. Pearson's correlation coefficient (r) is the best and most used correlation coefficient up to now. The correlation coefficient ranges between -1 and 1. In this paper, we have employed the cross-correlation technique used by Tsurutani et al⁴⁴, Panditet al⁴⁵ and Adhikari et al²³ to analyze and compare the correlation between Alfvén

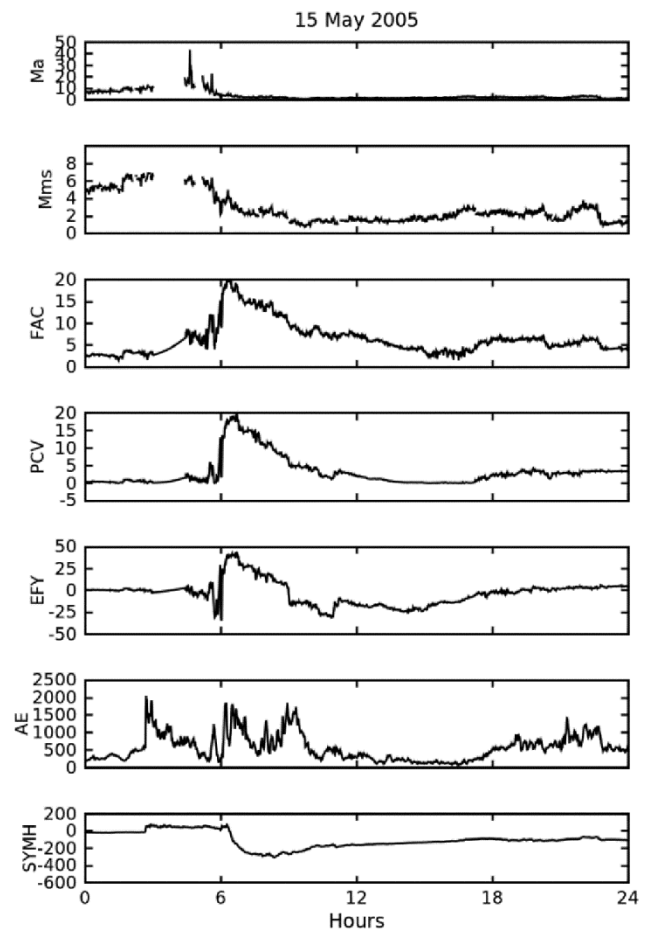


Fig. 8 — The different parameters are shown for 15 May 2005. From top to bottom: (a) Alfvén Mach number (M_A), (b) magnetosonic Mach number (M_{ms}), (c) field aligned current (FAC), (d) polar cap potential (PCV), (e) dawn dusk electric field (EFY), (f) AE index (nT), and (g) SYMH index (nT).

M_A and the parameters of FACs, PCV, and dawn-to-dusk IEF E_y . The timescale is used to determine the lead or lag between parameters at the time of correlation. Here, the sequential order, in which variables are used, determines the time scale. As all our major parameters (i.e., Alfvén M_A , FACs, PCV, dawn-to-dusk IEF E_y), which are denoted by IMF- E_y in the cross-correlation graphs, are related to solar wind, we expected some relation between them. In addition, we could see some relations among them through the help of cross correlation. Even though M_A is calculated from Band V_{sw} , we have carried our analysis to examine the variation of patterns during the quiet and extreme solar wind conditions.

In ICME driven event of 31 March 2001, Fig. 9 depicts the positive correlation between M_A and FAC with a coefficient of 0.8 with zero lag, whereas Korth et al⁴⁶ found no detectable dependence of FAC on

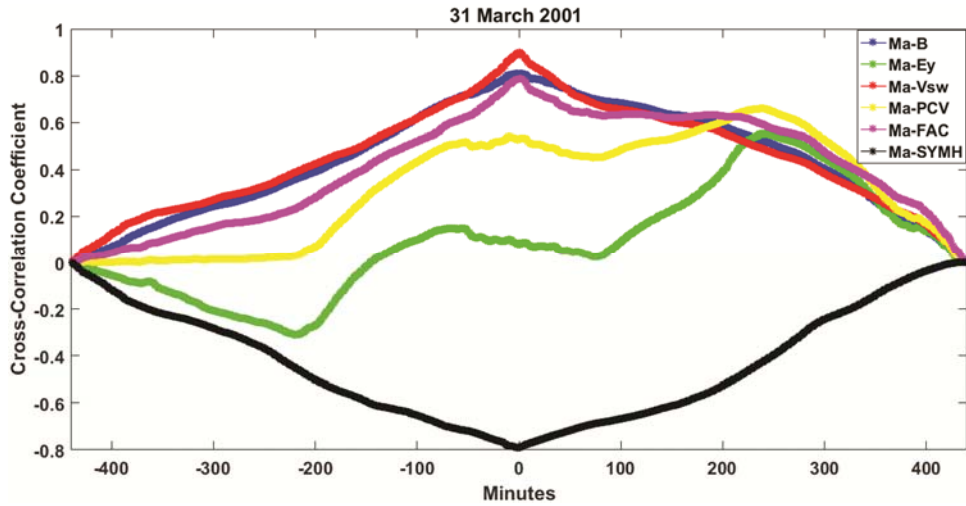


Fig. 9 — The line plots illustrate the cross-correlations of Alfvén Mach number (M_A) with B (blue), Ey (green), Vsw (red), PCV (yellow), FAC (pink), and SYMH (black) during 31 March 2001.

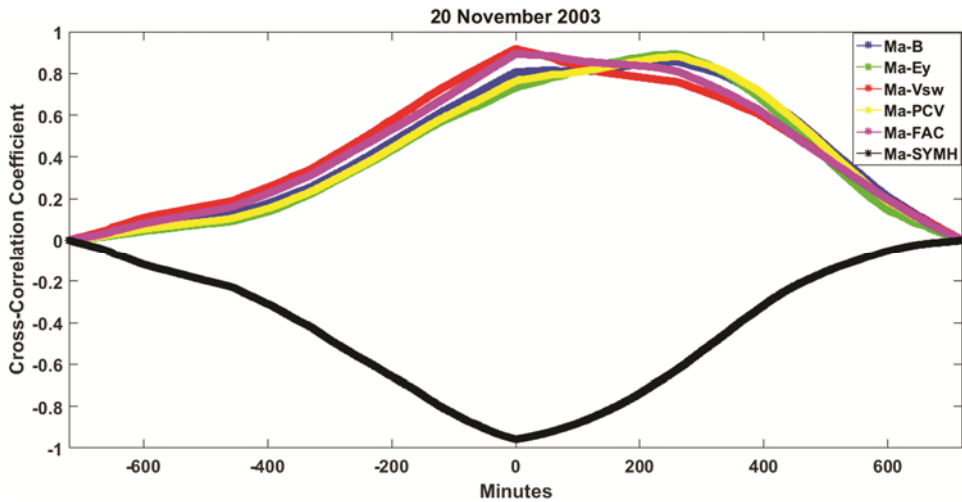


Fig. 10 — The line plots illustrate the cross-correlations of Alfvén Mach number (M_A) with B (blue), Ey (green), Vsw (red), PCV (yellow), FAC (pink), and SYMH (black) during 20 November 2003.

Alfvén M_A when normalizing the FAC to the median solar-wind electric field and dynamic pressure. Good anti-correlation of M_A and SYM-H was observed. But showed poor correlation of M_A with the IEF-Ey and had moderate relationship with PCV might be due to the unprecedented major storm. So, the solar energetic particles content in the interplanetary field was less and was not affected in a considerable amount by the solar wind following this ICME event. However, another ICME related event we observed was 20 November 2003, during which we found that M_A was in positive correlation with FAC and with no time lag. In addition, we also observed that M_A was in positive correlation with PCV and the Ey and with a time lag of $\sim +200$ min. This result was somewhat different

from the earlier ICME event of 31 March 2001 because the 20 November 2003 storm was led by another ICME event as well, thus, SEPs were greatly affected by the solar winds. Moreover, SYM-H was also in a negative correlation with M_A during this 20 November 2003 storm. We also studied one CIR event occurring on 15 May 2005 and we found expected results during this event as well. In our cross correlations, we observed positive correlation between M_A and FAC and PCV, whereas Ey was not in relation with M_A . All these relations occurred with a 0-time lag. In addition, like other geomagnetic events, SYM-H was in negative correlation with M_A with a ~ -50 min time lag. One distinct observation we made during the studying of these events was that

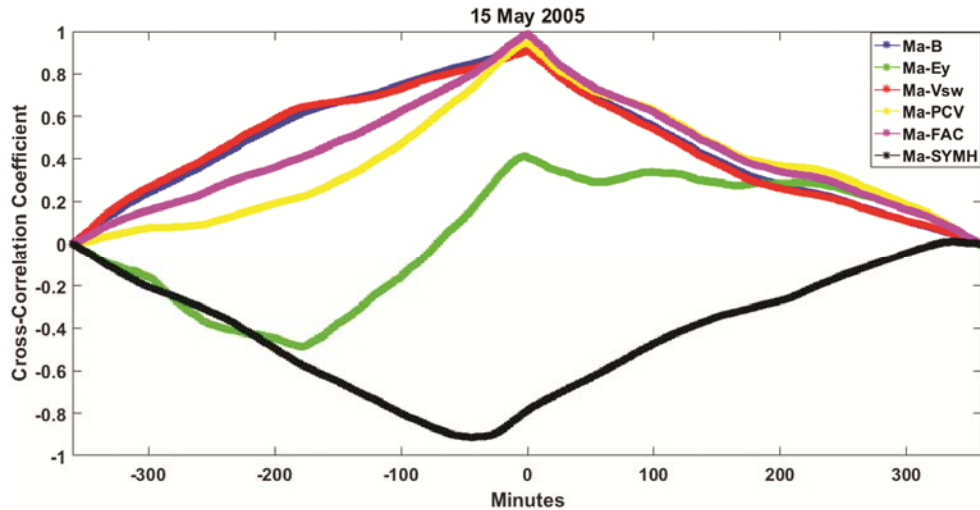


Fig. 11 — The line plots illustrate the cross-correlations of Alfvén Mach number (M_A) with B (blue), Ey (green), Vsw (red), PCV (yellow), FAC (pink), and SYMH (black) during 15th May 2005.

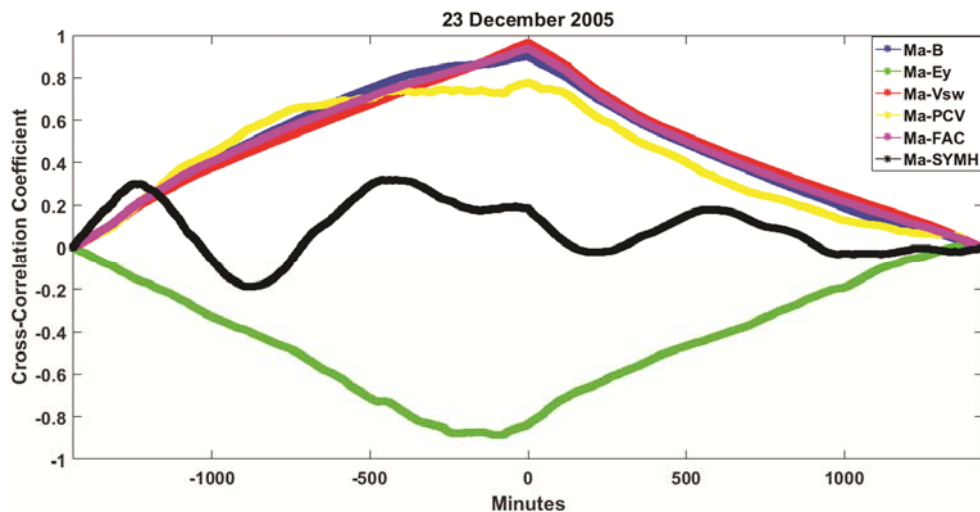


Fig. 12 — The line plots illustrate the cross-correlations of Alfvén Mach number (M_A) with B (blue), Ey (green), Vsw (red), PCV (yellow), FAC (pink), and SYMH (black) during 23 December 2005.

M_A , FAC, PCV, and Ey started showing some relation after the beginning of the initial phase. Before the initial phase, they showed no correlation. This also supports the fact that M_A , FAC, PCV and Ey are somehow governed by the solar wind condition.

However, we came across some unexpected results during the quiet day of 23 December 2005. In the cross-correlation figure of this event, we found out that M_A was in correlation with FAC and PCV and in no correlation with SYM-H. These were found, as expected, but we observed also that the IEF Ey was in a negative correlation with M_A with a ~ -100 minutes time lag. This was not a scientifically meaningful result. The result we obtained regarding Ey was due

to the presence and movements of SEPs leading to the solar-wind magnetosphere coupling, which was due to the viscous penetration and ionic penetration⁴⁷.

Correlation between M_A and other parameters such as PCV and IEF Ey is dependent on the nature of the storm which can be seen through the different results we obtained during two ICME events (on 31 March 2001 when M_A was in no correlation with PCV and Ey, and on 20 November 2003 when positive correlations between M_A and PCV and Ey were found). Here, the former event was not preceded by any other solar event, whereas the later was preceded by strong solar storms. In addition, for the quiet period of 23 December 2005, we found a negative

correlation between M_A and E_y due to the viscous penetration. From these, we can conclude that the conditions governing the variations of M_A , FACs, PCV, and IEF E_y during the storm periods investigated were somehow similar during the disturbed period and were closely related to the prevailing solar wind conditions. However, the viscous penetration during the quiet day led to some scientifically not meaningful results regarding the condition of E_y during the quiet period. All these correlations are further supported by our observational results and discussions documented in our previous study.

4 Conclusions

To unveil the subtlety in geomagnetic storms due to different solar events, we have analyzed the fluctuations of Alfvén Mach number associated with magnetic fields of different solar events. Geomagnetic storms are associated with solar wind conditions and reflect the features of CME, ICME, CIR, HSS etc. Often, the magnetic fields are crucial for identifying the behavior of geomagnetic storms. Furthermore, in this study, we have analyzed the solar wind variables such as M_A , large-scale FACs, PCV, and dawn dusk IEF E_y during different solar wind activities. The relations of Mach number with FACs, PCV and IEF E_y are not solely dependent on any solar wind parameter but are affected by various conditions prior, during, and post the storm events regarding their prevailing solar maxima or minima conditions, ICMEs or CIR driven storms etc. Furthermore, conclusions of this paper are as follows:

- (i) Prior to the arrival of interplanetary shock (IS), M_{MS} and M_A show good relationship with FAC, PCV, E_y , and solar wind parameters; as the space weather seems unperturbed.
- (ii) On average, the value of M_{MS} (~ 6) during Quiet event is like the average value (~ 6) of M_{MS} prior to the arrival of interplanetary shock of CIR and ICME events.
- (iii) After the arrival of IS: abrupt increase in M_A shows the flow of eastward magnetopause current. However, a rapid decrease in M_A value is observed with the increase in negative interval of SYMH, the compression of Earth's magnetosphere results in geomagnetic disturbance.
- (iv) During the main phase of geomagnetic storm on all events, cross-correlation analysis substantiates the result obtained with good correlation

coefficient of M_A with FAC, PCV and other parameters of solar wind, agrees with results of previous research. We found that there is zero-time delay of M_A with both V_{sw} and FAC on all events. However, correlation of M_A with E_y showed erratic.

- (v) On CIR event (15 May 2005): during the main phase of geomagnetic storm followed by recovery phase, the M_A value reaches lower (on average) to 1. Interestingly, however, there is sharp increase in M_A (~ 45) value during the arrival of IS which is even greater than the value of M_A during the Quiet event. Such shocks are very rare in near space weather environment and are momentary might be due to predominance of the solar maxima condition.

The positive correlations among the various parameters were due to the merging of two different ICMEs driven solar storms and consequential intense southward interplanetary magnetic field. The negative relationships among the selected parameters may have been due to the slow recovery of the IMF B_z component. Since, M_A is influenced by the variations in any components of the IMF, so, the delay in IMF B_z recovery can be a scientifically meaningful reason of negative correlation among these parameters. The negative correlations observed between the Mach number and the IEF E_y could be due to the viscous and ionic penetrations too. We also conclude that the preceding solar wind could have vast effect on the variance of M_A of a geomagnetic event, in turn might have its effect on FACs, PCV, E_y , and also in other solar wind parameter.

Acknowledgements

We are grateful to the OMNI database for providing the data. The interplanetary magnetic field magnitude data, solar wind parameters' data, and data for the Mach numbers for this study were obtained from <https://omniweb.gsfc.nasa.gov/>. The authors would like to acknowledge Dr. Ildiko Horvath for providing the invaluable suggestion.

References

- 1 Russell C T & Vaisberg O, *Venus*, (1983) 873.
- 2 Chapman S & Bartels J, *Geomagnetism Volume II: Analysis of the Data, and Physical Theories*, Oxford University Press, (1940).
- 3 Gonzalez W D, Joselyn J A, Kamide Y, Kroehl H W, Rostoker G, Tsurutani B T & Vasyliunas V M, *J Geophys Res: Space Phys*, 99(A4) (1994) 5771.

- 4 Cloutier P A & Anderson H R, *Space Sci Rev*, 17(2-4) (1975) 563.
- 5 Iijima T & Potemra T A, *J Geophys Res*, 81(34) (1976b) 5971.
- 6 Chun F K & Russell C T, *J Geophys Res: Space Phys*, 102(A2) (1997) 2261.
- 7 Chapagain N, *Journal of Institute of Science and Technology (JIST)*, 20 (2) (2015) 84.
- 8 Papitashvili, V O, Rich F J, Heinemann M A & Hairston M R, *J Geophys Res: Space Phys*, 104(A1) (1999) 177.
- 9 Siscoe G L, Crooker N U & Siebert K D, *J Geophys Res: Space Phys*, 107(A10) (2002) SMP-21.
- 10 Hairston, M R, Hill T W & Heelis R A, *Geophys Res Lett*, 30(6) (2003).
- 11 Pedatella N M, Forbes J M & Richmond A D, *J Geophys Res: Space Phys*, 116 (2011).
- 12 Adhikari B, Baruwal P & Chapagain N P, *Earth Space Sci*, 4(1) (2017a) 2.
- 13 Mishra R K, Adhikari B, Pandit D & Chapagain N P, *Characteristic of Solar Wind Parameters and Geomagnetic Indices during Solar Flares*, Long-Term Datasets for the Understanding of Solar and Stellar Magnetic Cycles Proceedings IAU Symposium No. 340, (2018).
- 14 Boyle C B, Reiff P H & Hairston M R, *J Geophys Res: Space Phys*, 102(A1) (1997) 111.
- 15 Antonova E E & Ganushkina N Y, *Eur. Space Agency Spec Publ SP*, 389 (1996) 43.
- 16 Barbosa D D & Kivelson M G, *Geophys Res Lett*, 10(3) (1983) 210.
- 17 Chapman J F & Cairns I H, *J Geophys Res: Space Phys*, 108 (A5) (2003).
- 18 Eriksson S & Rastätter L, *Geophys Res Lett*, 40 (2013) 1257.
- 19 Lavraud B, Larroque E, Budnik E, Génot V, Borovsky J E, Dunlop M W & Ruffenach A, *Space Phys*, 118(3) (2013) 1089.
- 20 Iijima T & Potemra T A, *Geophys Res Lett*, 9(4) (1982) 442.
- 21 Kasran F A M, Jusoh M H, Adhikari B & Ab Rahim S A E, *J Phy: Conference Series*, 1152, (2019) 012027.
- 22 Wilder F D, Eriksson S, Korth H, Baker J B H, Hairston M R, Heinselman C & Anderson B J, *Geophys Res Lett*, 40 (2013) 2489.
- 23 Adhikari B, Dahal S, Sapkota N, Baruwal P, Bhattarai B, Khanal K & Chapagain N P, *Earth Space Sci*, 5(9) (2018) 440.
- 24 Spreiter J R, Summers A L & Alksne A Y, *Planet Space Sci*, 14(3) (1966a) 223.
- 25 Biernat H K, Erkaev, N V, Farrugia C J, Vogl D F & Schaffnerberger W, *Nonlinear Process Geophys*, 7 (2000) 201.
- 26 Borovsky J E & Denton M H, *J Geophys Res*, 111 (2006a) A07S08.
- 27 Gosling J T, *Geophys. Monogr. Ser.*, 58 (1990) 343.
- 28 Fairfield D H, Iver H C, Desch M D, Szabo A, Lazarus A J & Aellig M R, *J Geophys Res*, 106 (2001) 361.
- 29 Merka J, Szabo A, Slavin J A & Peredo M, *J Geophys Res* 110 (A4) (2005) 4202.
- 30 Wang J, Guo Z, Ge Y S, Du A, Huang C & Qin P, *J Space Weather and Space Clim*, 8 (2018) A41.
- 31 Moon G H, *J Astron Space Sci*, 29(3) (2012) 259.
- 32 Sundberg T, Burgess D, Scholer M, Masters A & Sulaiman A H, *The Astrophysical Journal*, 836(1) (2017).
- 33 Jankovicova D, Dolinsky P, Valach F & Voros Z, *J Atmos Sol Terr Phys*, 64 (2002) 651.
- 34 Echer E, Gonzalez W D, Vieira, L E A Dal Lago A, Guarnieri F L, Prestes A, Gonzalez A L C & Schuch N J, *Braz. J Phys*, 33(1) (2003) 115.
- 35 Weimer D R, *J Geophys Res: Space Phys*, 106(A7) (2001) 12889.
- 36 Adhikari B, Dahal S & Chapagain N P, *Earth Space Sci*, 4(5) (2017b) 257.
- 37 Kakad B, Kakad A, Ramesh D S & Lakhina G S, *J Space Weather and Space Clim*, 9 (2019).
- 38 Shepherd S G, *J. Atmos Sol Terr. Phys*, 69(3) (2007) 234.
- 39 Adhikari B & Chapagain N P, *Journal of Nepal Physical Society (JNPS)*, 3(1) (2015) 6.
- 40 Subedi A, Adhikari B & Mishra R K, *Himalayan Physics*, (2017) 80.
- 41 Katz R W, *J Climatol*, 8(3) (1988) 241.
- 42 Vichare G, Rawat R, Hanchinal A, Sinha A K, Dhar A & Pathan B M, *Earth planets space*, 64(11) (2012) 1023.
- 43 Usoro A E, *J Statistical and Econometric Methods*, 4(1) (2015) 63.
- 44 Tsurutani B T, Gould T, Goldstein B E, Gonzalez W D & Sugiura M, *J Geophys Res: Space Phys*, 95(A3) (1990) 2241.
- 45 Pandit D, Chapagain N P, Adhikari B and Mishra R K, *Activities, and Its Impact on Space Weather*, Long-Term Datasets for the Understanding of Solar and Stellar Magnetic Cycles Proceedings IAU Symposium No. 340, (2018), doi:10.1017/S1743921318001308.
- 46 Korth H, Anderson B J & Waters C L, *Ann Geophys*, 28(2) (2010).
- 47 Baumjohann W, *Solar wind-magnetosphere coupling*, (1986) 3.